18th Australasian Fluid Mechanics Conference
Launceston, Australia
3-7 December 2012

Elite Cycling Aerodynamics: Wind Tunnel Experiments and CFD

M. D. Griffith, T. Crouch, M. C. Thompson, D. Burton and J. Sheridan

Department of Mechanical & Aerospace Engineering, Monash University, Victoria 3800, Australia

Abstract

An experimental and numerical study of the aerodynamics of a cyclist in a typical racing position is presented. The study aims to provide understanding of the fundamental aerodynamic characteristics which underpin variations of drag with changes to rider shape and position. Experimentally, for a mannequin (with static crank/leg position) in a wind tunnel, velocity fields at several streamwise stations are measured by traversing the plane with a probe. The structure of the wake depends strongly on the leg position, is associated with the flow around the hips and can lead to large variations in the drag. Numerically, the same mannequin geometry is modeled and the flow simulated using a commercial fluid flow solver (ANSYS–CFX). Similar variation with crank angle of drag and flow topology is observed. Transient flow simulations are found to match better with the mean velocity experimental measurements. It is found that for some crank angles, the wake is defined by a relatively strong vortex pair, and for others the wake is more oscillatory.

Introduction

Cycling at high speeds, such as in racing, the aerodynamic drag can account for up to 90% of the resistance experienced by the cyclist[1, 4]. The drag force, D is described by:

$$D = 0.5\rho U^2 C_D A, \tag{1}$$

where ρ is the density of air, U is the cyclist velocity, C_D is the coefficient of drag and A is the frontal area of the cyclist. At high speed, the cyclist can reduce the drag experienced by minimizing frontal area, A, or by configuring their position to achieve a flow minimizing drag coefficient, C_D. Any approach taken must be balanced with the optimal rider position for power output, as well as being within the rules set by the competition regulators.

There is only limited work on cyclist aerodynamics using computational fluid dynamics in the literature. Defraeye, Blocken, Koninckx, Hespel and Carmeliet[5] have analyzed the flow past a rider at fixed leg position without bike using CFD, employing both steady-state RANS and transient LES turbulence models. They found agreement with their wind tunnel experiments, but limited their comparisons to pressure tap measurements on the rider surface, without examining the wake flow structure.

To inform strategies for reducing drag, this study seeks to further understanding of the factors influencing C_D, namely the fluid dynamics, using both wind tunnel observations and numerical simulation. The study builds upon recent wind tunnel measurements performed within the research group[2, 3]. The paper seeks to find strong comparisons between numerical and experimental data, so to better characterize the fundamental flow features of a cyclist wake and how these effect aerodynamic drag.

Method

All flows were run with a freestream velocity $U = 16$ m/s, or 57.6 km/h. The model of the cyclist was based on a typical track bike with a cyclist in a static racing position; figure 1 shows the two experimental and numerical models tested. For the wind tunnel experiments, a mannequin was produced which provided rotation at the hips and knees, allowing the full range of crank positions to be tested. Crank angles were measured with the reference (crank angle, $\theta = 0$) located where the left foot is at its furthest downstream position, or, where the pedals are level and the right foot is towards the front of the bike. In the streamwise or x direction, $x = 0$ is defined as co-located with the rear axle of the bicycle. The bicycle consisted of a carbon fibre Bike Technologies (BT) frame, fitted with Shimano wheel rims.

Figure 1: The two cyclist models employed. At top, the mannequin used in the wind tunnel experiments, and at bottom a sketch of the cyclist model used in the numerical simulations.

Experiments were carried out in the Monash Large Wind Tunnel at Monash University. Measurements of the time-averaged three component velocity field were taken using a four hole dynamic pressure probe, commonly referred to as a Cobra probe. The position of the probe was controlled with a two axis traverse. Measurements were taken on and behind the body of the cyclist in planes perpendicular to the direction of flow, with each measurement sampled at 1250Hz for 15 seconds. A six component kistler force balance of the piezoelectric type was employed, which enabled the measurement of drag and lift forces experienced by the model. The force balance was positioned beneath the wind tunnel floor; struts were used on the front and rear axles to firmly fix the model. Force measurements were taken as the mean of three separate tests sampled at 500 Hz for 30 seconds. The model was placed on a raised box with a cantilevered splitter on the leading edge to limit the effect of the raised box and the floor boundary layer on the flow and measurements.

Numerically, flows were simulated using ANSYS–CFX. The numerical model of the rider was created from the dimensions of the experimental mannequin, while the head and helmet were taken from a scan. Some details of the experimental model were not recreated exactly, with the muscled mannequin arms being depicted with simpler tapered cylindrical and elliptical sections. A small stand near the rear axle, used to hold the experimental model in a stable vertical position was not included in the numerical model. For the bicycle, a generic model was created based on the major dimensions of a typical track bicycle. Wheel spokes were not included. Meshes were constructed over the

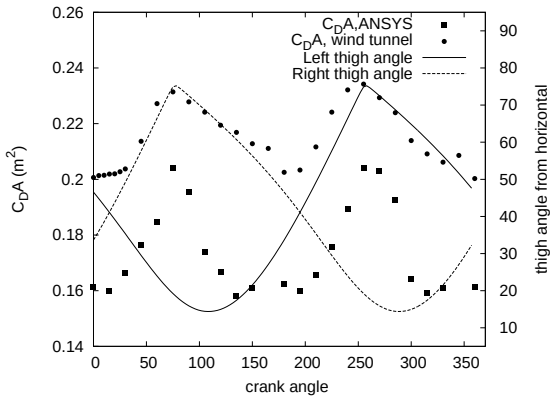

Figure 2: Plot of C_DA against crank angle for both wind tunnel measurements and ANSYS numerical simulations (points). Also plotted are the angles of each of the thighs through the crank angle cycle (lines).

range of crank angles, with each consisting of approximately 25 million elements.

The numerical results presented in this paper were taken using both steady-state and transient simulations. For steady-state, the Shear Stress Transport (SST) turbulence model is best suited for strongly three-dimensional separated flow, such as seen in the flow over a cyclist. For similar reasons, for transient solutions, the Scale-Adaptive Simulation Shear Stress Transport (SAS-SST) model[6] was judged to be most suitable. All solutions were iterated until the root-mean-squared residual quantities were of the order of 10^{-5}. A grid resolution study was undertaken, whereby resolution of the surface elements on the rider surface was increased. No change greater than 1% in measured mean lift or drag forces was found at resolutions higher than that used for the results presented here, for both steady and transient simulations. For transient simulations, a timestep of 5×10^4 seconds was employed; timestep sensitivity was tested down to a timestep of 1×10^4 and no appreciable difference was observed in either the mean or transient behaviour of the force measurements or averaged vorticity fields.

Results

Figure 2 plots the measured drag in both the experiments and numerics. Due to the changing frontal area of the geometry through the crank angle cycle, in this paper the quantity of drag coefficient times area, C_DA, is used to represent the drag on the cyclist; namely $C_DA = \frac{D}{\frac{1}{2}\rho U^2}$, where D is the drag force and ρ is the density of the fluid. From figure 2, it is apparent that the numerical model underpredicts the C_DA compared to the experimental model. There are several possible explanations for this: firstly, the geometry used in the numerical model does not match exactly the model used experimentally; there are numerous small differences, such as the presence of a stand on the rear axle to hold the experimental model in place. The bicycle of the numerical model is of a simpler design than that used experimentally; there has not been an exact replication of the handle bars in the numerical model, nor have wheel spokes been included. All of these small modifications have small effects; however, cumulatively, they may represent a significant difference in the measured drag.

Other than differences in the geometry, the discrepancy in C_DA may also come down to the numerical difficulties in simulating a turbulent flow with a highly three-dimensional geometry, for a Reynolds number of the order of 10^6. A further consideration is that the numerical results plotted in figure 2 have been obtained using a steady-state numerical solver, whereas the experimental measurements are mean values. The numerical solver iterates towards a particular solution, not the mean of a time-dependent solution. Results of transient simulations are shown later in this paper.

A good comparison that can be made lies in the variation of the measured values of C_DA with crank angle, which the numerical simulations predict well. A minimum in drag is observed for crank angles of 15 and 195 degrees; geometrically, these are the angles at which the left and right thigh of the rider are evenly aligned (see the bottom right image of figure 1). The maxima in drag occur at crank angles of 75 and 255 degrees; these are the positions where one of the legs is almost straight and the other is folded up. Since figure 2 presents values of C_DA, there is a question over whether the variation seen is based on changes in the flow (C_D) or in the change in frontal area of the geometry (A). Though not shown here, the frontal area of the geometry varies through the crank cycle. Its variation only accounts for approximately half of the variation in C_DA seen in figure 2, indicating that a large proportion of the variation is due to changes in the wake flow with crank angle.

Also plotted on figure 2 is the angle of each thigh from the horizontal as it varies throughout the crank angle cycle. The maxima of this angle (which indicate a straightening leg) match up closely with the maxima in C_DA. The outstretching of one leg appears to lead not only to an increase in frontal area, but also an increase in drag coefficient, C_D.

To visualize the changes in wake flow structure responsible for the variation in C_DA over the crank angle cycle, figures 3 and 4 plot contours of vorticity at several planes in cross-section to the direction of the flow, for the experimental and numerical data sets and for crank angles of 15 and 75 degrees. Regarding the results obtained with the SST model, of note is that averaged mean vorticity contours for the wind tunnel results are being compared with numerical solutions obtained with the steady-state solver. The 15 degree crank angle case in figure 3 does not provide a good comparison. The experimental result (at right) is symmetric, while the steady-state numerical result (at left) is biased to one side. Additionally, the C_DA for the 15 degree case did not converge to as high an accuracy as for some other crank angles; indeed, if the vorticity is allowed to iterate further the alignment of the wake can deflect in the other direction, indicating a time-dependent flow. If this is the case, the usefulness of the steady-state numerical simulation is limited; the experimental result may represent an average of a "flapping" of the wake from one side to the other.

The plots for the 75 degree crank angle case in figure 4 show a more consistent bias to one side. In all the numerics and in the experimental measurements for this case, the flow is deflected to the side of the domain corresponding to the side with the straight leg. In this configuration, the straight leg produces a cavity of sorts in the side of the geometry, as compared to the side where the leg is folded up close to the chest. The geometry itself becomes significantly more asymmetric than in the 15 degree case, and this is reflected in the wake flow.

The usefulness of the steady-state numerical simulations is limited if the flow is significantly time-dependent. Therefore, transient simulations have been run for the two main cases of interest, crank angles 15 and 75 degrees (the low and high drag case). These simulations take approximately 30 to 40 times longer to run than the steady state simulations, so the transient simulations have been limited to these two cases.

For the 15 degree case, the average vorticity field taken from the transient simulation (middle column of figure 3) gives a better comparison to the wind tunnel measurements. Essentially the same vorticity structure is seen at $x = 0.32$ m for both the ex-

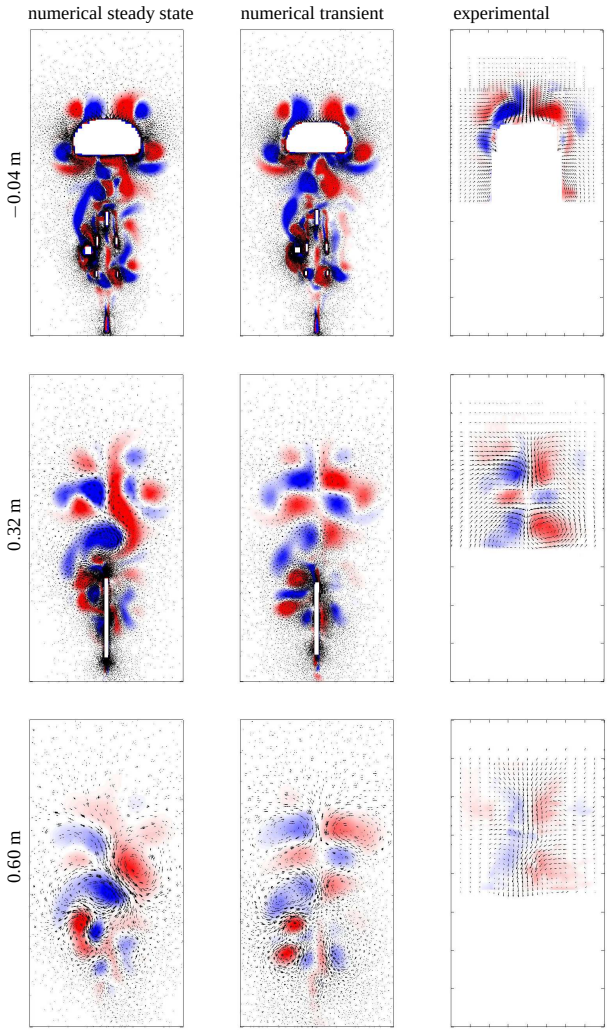

Figure 3: Contours of streamwise vorticity with vectors of cross-stream velocity, for a cyclist at crank angle of 15°, at cross sections $x = -0.04$ m (top), 0.32 m (middle) and 0.6 m (bottom), for both numerical steady-state (left), numerical transient (middle) and experimental (right) results. Contours vary across the range $-100s^{-1} \leq \omega_x \leq 100s^{-1}$.

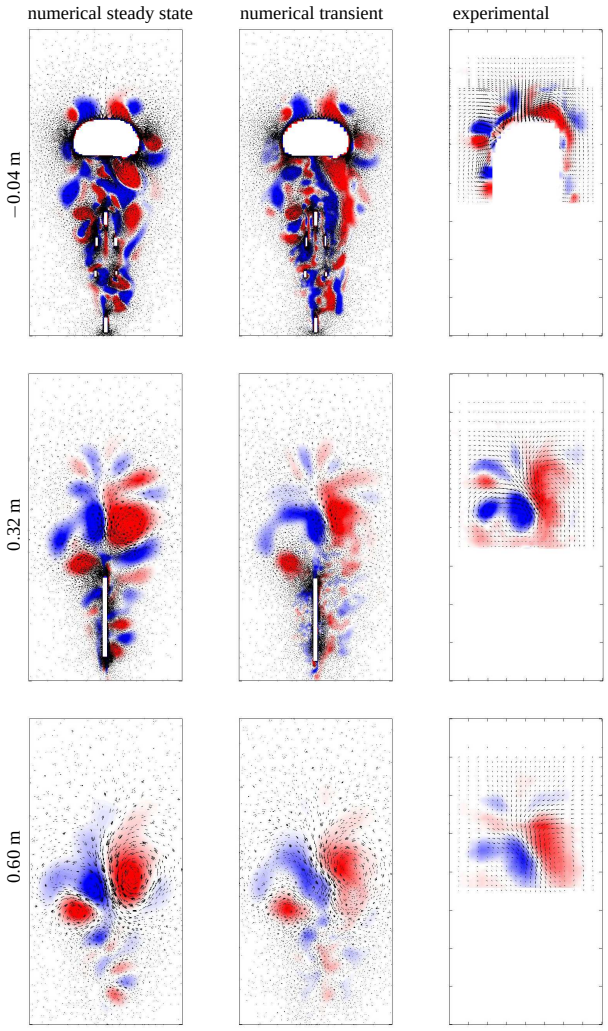

Figure 4: Contours of streamwise vorticity with vectors of cross-stream velocity, for a cyclist at crank angle of 75°, at cross sections $x = -0.04$ m (top), 0.32 m (middle) and 0.6 (bottom), for both numerical steady-state (left), numerical transient (middle) and experimental (right) results. Contours vary across the range $-100s^{-1} \leq \omega_x \leq 100s^{-1}$.

perimental and transient numerical results; at $x = 0.60$ m, the vorticity structure persists in the numerical case, but the experimental result is less well-defined. The instantaneous fields of vorticity (as shown later in figure 5) do not closely resemble the averaged field; the wake flow oscillates from one side of the rider to the other, and the experimental and transient numerical results of figure 3 show the symmetric average of this oscillation.

Regarding the comparisons for the 75 degree crank angle case in figure 4, although the steady-state numerical simulation matches well with the experimental observation, the transient simulation is an improvement. The same settling of the wake flow to the side of the outstretched leg is evident. In contrast to the 15 degree state, the steady-state simulation compares well with the experiment, indicating that the flow is not as strongly time-dependent and that stronger more well-defined vorticity structures exist. Indeed, the instantaneous fields of vorticity for the 75 degree case (an example of which is found in figure 5) exhibit the same sideways bias as seen in figure 4, as well as the two main concentrations of positive and negative vorticity evident at the $x = 0.32$ m and 0.60 m planes.

The two crank angle cases of 15 and 75 degrees were chosen as they are representative of the low and high drag cases evident in figure 2. With a difference in C_DA, a difference should exist in the velocity defect in the wake flow of each case; or, a difference in the amount of energy in the wake flow of each case. This can be seen qualitatively in figure 5, which plots contours of streamwise vorticity in the wake of the cyclist for both the 15 and 75 degree cases, taken from the transient numerical simulations. The stronger velocity defect is evident for the 75 degree crank angle case and appears to be centered on the main negative-positive vorticity concentrations of figure 4. The large area of reduced streamwise velocity component in the high-drag 75 degree crank angle case is also apparent in the instantaneous velocity fields, which are shown in figure 5. Even in the instantaneous field, the flow for 75 degree crank angle exhibits a relatively well-defined vortex pair, in contrast with the flow for 15 degrees.

As well as the mean quantities, the transient behaviour of the flow is also of interest. Figure 6(a) plots time series of u, v and w velocities for a probe placed in the wake for the 15 degree crank angle case, at $x = 0.32$, $y = 1.0$ and $z = 0$, or, around the midpoint of the middle image of figure 3. The signals contain

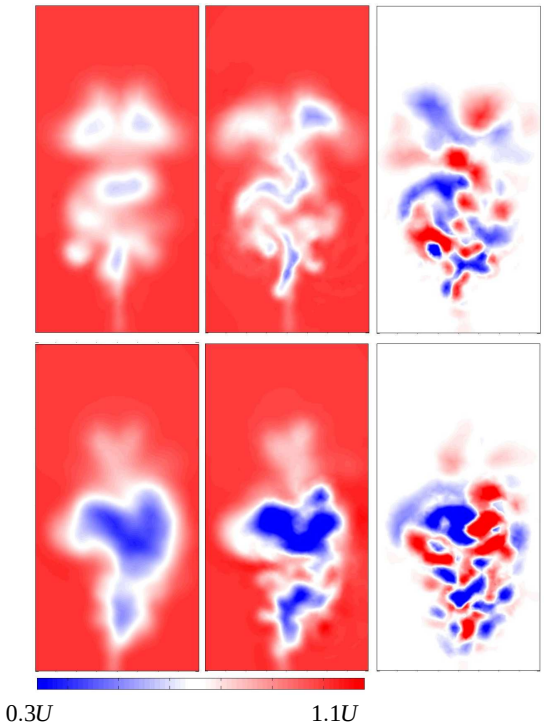

Figure 5: At left, contours of streamwise velocity in a plane located at $x = 0.60$ m, for the 15 (top) and 75 (bottom) degree cases. Middle, the same contours but for an instantaneous field. At right are the corresponding instantaneous streamwise vorticity contours, for the same levels as in figures 3 and 4.

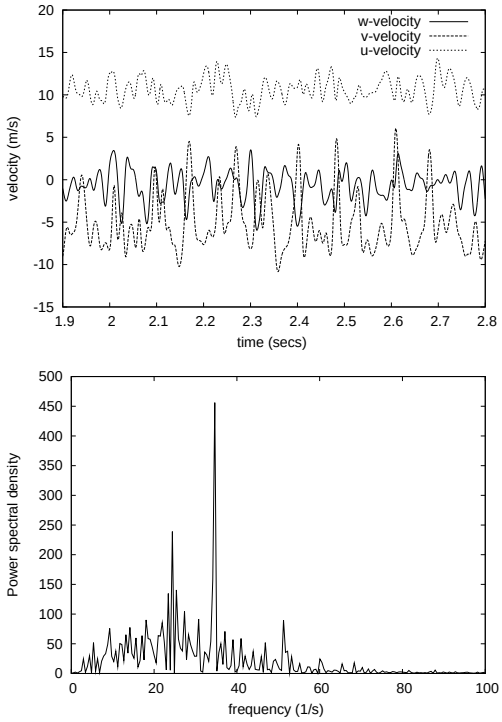

Figure 6: (a) Time series of the cross-stream u- and v-velocity and the streamwise w-velocity components, taken at $x = 0.32$, $y = 1.0$ and $z = 0$, for the 15 degree case; (b) corresponding power spectrum for the cross-stream (horizontal) u-velocity component.

high frequency oscillations. Figure 6(b) plots the corresponding power spectrum for the horizontal cross-stream u-velocity. The spectrum exhibits a strong peak at approximately 34Hz. Further work is ongoing on other frequencies in the flow, throughout the wake, which may give further information on the wake fluctuations.

Of importance is the question of relevance for the flow past a cyclist with rotating legs, of whether a quasi-steady assumption is valid. The frequencies observed so far in the flow past the static mannequin are greater than the frequencies associated with pedaling under racing conditions (approximately 2 Hz). The speed of the oncoming flow, U, is also far greater than the speed of the moving legs. Furthermore, by running transient simulations, it is observed that some flow features, such as the drag and lift, settle into their steady state within 0.1 to 0.2 seconds. Nonetheless, this is an assumption which will need to be tested further and is the subject of ongoing work.

Conclusions

This paper has presented numerical and experimental data on the flow past a model of a racing cyclist, over a range of static leg positions. In all data sets, a dependence of drag on crank angle was observed, with high drag measurements corresponding with rider geometries with one leg extended to nearly full length and the other folded up close to the torso. The low drag case corresponds to the rider position where both thighs are at the same angle. Numerically, transient simulations were found to provide the best flow field comparisons with the experimental results. A shifting of the wake flow to one side for the high drag cases was observed, while for the low drag case, a weakly defined wake structure was observed, the average of which lead to a nearly symmetric flow field. The implication for further CFD work is that, depending on crank angle, steady-state simulations may not capture all of the flow features.

This work was supported by the Australian Research Council, through the Linkage Project scheme (project number: LP100200090).

References

[1] Grappe, G. and Candau, R. and Belli, A. and Rouillon, J. D, Aerodynamic Drag in Field Cycling with Special Reference to the Obree's Position, *Ergonomics*, **40**, 1997, 1299–1311.

[2] Crouch, T. N. and Thompson, M. and Burton, D. and Sheridan, J. and Brown, N. A. T., Dominant Flow Structures in the Wake of a Cyclist, 30th AIAA Applied Aerodynamics Conference, New Orleans, USA, 2012.

[3] Crouch, T. and Sheridan, J. and Burton, D. and Thompson, M. and Brown, N. A. T., A Quasi-static Investigation of the Effect of Leg Position on Cyclist Aerodynamic Drag, 9th Conference of the International Sports Engineering Association, Lowell, USA, 2012.

[4] Kyle, C. R. and Burke, E. R., Improving the Racing Bicycle, *Mechanical Engineering*, **105 (9)**, 1984, 34–35.

[5] Defraeye, T. and Blocken, B. and Koninckx, E. and Hespel, P. and Carmeliet, J., Aerodynamic Study of Different Cyclist Positions: CFD Analysis and Full-scale Wind-Tunnel Tests, *J. Biomechanics*, **43**, 2010, 1262–1268.

[6] Menter, F. R. and Egorov, Y., The Scale-Adaptive Simulation Method for Unsteady Turbulent Flow Predictions. Part 1: Theory and Model Description, *Flow Turb. Comb.*, **85**, 2010, 113–138.